Radiation-Induced Defects in Glasses: Origin of Power-Law Dependence of Concentration on Dose

D. L. Griscom, M. E. Gingerich, and E. J. Friebele
Optical Sciences Division, Naval Research Laboratory, Washington, D.C. 20375
(Received 17 May 1993)

We propose, and verify in the case of a Ge-doped-silica-core optical fiber, a general explanation for the power-law dependencies on dose frequently observed for the concentrations of radiation-induced defect centers in insulating glasses. This insight permits *detailed prediction* of the postirradiation recovery curves, given just the empirical exponent of the power law, $0<f<1$, and the experimental irradiation time, t_{irrad}. The time constant of the recovery is given by $t_{\text{irrad}}/(1-f)$, independent of the order of the kinetics. We establish a microscopic model (radiolytic oxygen molecules) for the γ-ray-induced absorption at 1.3 μm in our test fibers and infer a diffusion-limited bimolecular recombination process.

PACS numbers: 61.72.Cc, 42.70.Ce, 61.43.Fx, 82.50.Gw

Analyzed data on thousands of condensed matter samples and tens of relaxation phenomena have appeared to be described by a single "universal" relation [1-3],

$$q(t)=q_0\exp[-(t/\tau)^{\alpha}], \tag{1}$$

where $q(t)$ is the measured quantity, τ is the observed time constant, and α is a number between 0 and 1. Over the years, there has been intense interest in developing evidence for the microscopic physics underlying the data described by this otherwise phenomenological equation. Nominally, two classes of mechanisms are considered: (i) diffusion-controlled reactions in which the "stretched exponential" behavior is attributed to random distributions in the parameters governing transport in disordered solids and (ii) hierarchically limited dynamics resulting in correlated relaxation processes consisting of several successive steps [4]. Among the relaxation phenomena recently interpreted in terms of Eq. (1) are the long-term kinetics of postirradiation thermal bleaching of radiation-induced defects in glasses [5].

A separate phenomenon has often been reported in the literature [6-11], usually, though not always [11], without any attempt at interpretation. This phenomenon is defect growth kinetics taking the form

$$q=CD^{f}, \tag{2}$$

where D is the radiation dose and C and f (<1) are empirical constants. Many of the published power-law growth curves have been recorded for the induced attenuations in optical fibers [9,10]. In each of these cases, the postirradiation thermal decay of the attenuation has exhibited "stretched" behaviors which we have previously opted to fit to standard nth order kinetic formulations —rather than Eq. (1)—i.e., solutions of

$$dq/dt=-Rq^{n}, \tag{3}$$

where R is a constant. Our prior fits [9,10] implied effective values of n ranging from 3 to 10, despite our belief that the underlying kinetics must be bimolecular (as for recombination of electrons and holes or vacancies and interstitials).

In the present paper we now prove that the oft-observed power-law growth and "stretched" ($n>2$) decay behaviors of Eqs. (2) and (3), respectively, are simultaneously interpretable in terms of standard bimolecular kinetics ($n=2$) if we decompose the observed kinetic curves into the contributions of a distribution of independent defect subpopulations, each characterized by a different production rate constant K and a recombination rate constant R related to K by a semiempirical formula. We use our model to analyze new experimental data for the ^{60}Co-γ-ray-induced attenuation measured at 1.3 μm in an optical fiber [12] with a Ge-doped-silica core and a pure silica cladding.

We begin our analysis by differentiating Eq. (2) to obtain an empirical growth rate equation

$$dq/dt=CfD^{f-1}\dot{D}, \tag{4}$$

where $\dot{D}$ is the dose rate. In classical nth order kinetics, a rate equation of the following form always applies:

$$dq/dt=K\dot{D}-Rq^{n}. \tag{5}$$

We now equate the right-hand sides of Eqs. (4) and (5) to obtain

$$R=q^{-n}(K-CfD^{f-1})\dot{D}. \tag{6}$$

Equation (6) shows that for a power-law growth curve, the effective "constants" R and K must be empirically interrelated and depend on D, $\dot{D}$, q, and n. In our model, we posit that the underlying classical rate constants are time invariant. This ansatz leaves us with no choice but to treat the empirical growth curve as the envelope of a series of discrete classical curves (or integration over a continuum of curves) given by the solutions of Eq. (5) for a range of *dose independent* values of K_i and interrelated values of R_i. It is useful for heuristic purposes to attach a value of K_i to each point on the empirical growth curve according to the equations $q_{(i)}=K_iD_{(i)}=CD_{(i)}^{f}$ (an approximation which assumes that the ith component curve saturates abruptly when it reaches the empirical curve at coordinates $D_{(i)}$, $q_{(i)}$). In this way, we can eliminate either $D_{(i)}$ and $q_{(i)}$ or K_i and $q_{(i)}$ from Eq. (6). For

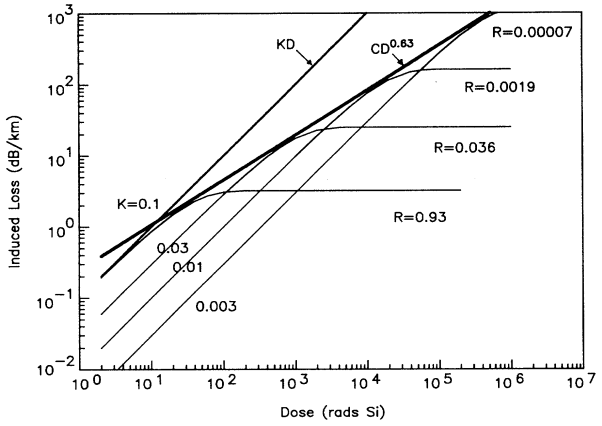

FIG. 1. An experimental power-law growth curve, Loss $=CD^{0.63}$, is modeled as the envelope of an ensemble of saturating exponentials characterized by correlated production- and recombination-rate constants K_i and R_i, respectively. In this first-order-kinetic analysis, the steady-state (saturation) losses are given by $K_i\dot{D}/R_i$, where $\dot{D}$ is the dose rate.

present purposes, we now assume the expected kinetic order ($n=2$) in performing both of these eliminations, illuming first the dependence of R_i on K_i,

$$R_i = K_i^{(1+f)/(1-f)} C^{2/(f-1)} (1-f)\dot{D}\,, \tag{7}$$

and second the dependence on dose [13] of the instantaneously measurable R_i,

$$R_i = C^{-1} D_{(i)}^{-(f+1)} (1-f)\dot{D}\,. \tag{8}$$

We have also derived the corresponding relations for first-order kinetics and, since the $n=1$ solutions of Eq. (5) are well known, we have used these relations in Fig. 1 to perform a coarse decomposition of an empirical power-law growth curve according to our model premise. We will demonstrate below that such a scheme (presumably based on $n=2$ solutions) [14] can uniquely account for our data.

Returning to Eq. (8), we see that our model makes a no-adjustable-parameters *prediction* of the recovery curves to be expected when the radiation is interrupted. The only knowledge required consists of the empirical growth parameters C and f, the dose rate $\dot{D}$, and the final accumulated dose $D_{(i)}=D_{\text{cum}}$. To test this prediction in the case of the present experiment, we use the standard nth order kinetic solution for $n>1$:

$$q(t) = q_0[1+(n-1)q_0^{n-1}Rt]^{1/(1-n)}\,, \tag{9}$$

taking $q_0 = C(D_{\text{cum}})^f$ and $R=R_i$ as given by Eq. (8) when $D_{(i)}=D_{\text{cum}}$.

For a variety of dose rates (experimentally resulting in different values of both C and f) and several different cumulative doses, the "simple" recovery curves calculated via Eq. (9) using $n=2$ gave the experimentally correct half life, though they did not reproduce the "stretched" experimental curves, which were better fit by using $n\approx 5$–6. However, the present model envisions the empirical growth curve to consist of a *summation* of individual curves, as illustrated in Fig. 1. Thus, to be consistent, a *detailed* model prediction of the recovery curve must comprise a summation of decay curves, e.g., with values of $q_{0(i)}$ which can be picked graphically from Fig. 1 as the values of the ith component curve evaluated at $D=D_{\text{cum}}$. [Of course, the decay rate constants R_i to be used are those calculated from Eq. (7) and not the $n=1$ rates of Fig. 1.] The results achieved in this way are illustrated in Figs. 2(b) and 3(b), where the symbols are data and the curves are *predictions* (not fits) [15]. *The astonishing predictive ability of the theory at once proves*

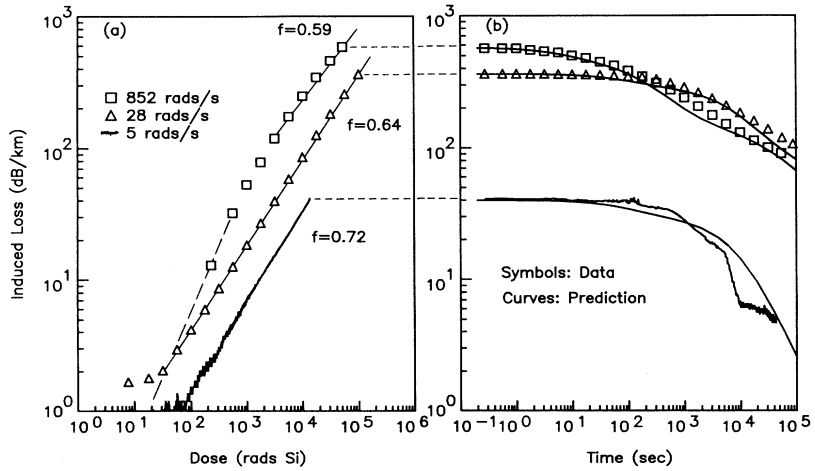

FIG. 2. γ-ray-induced losses at 1.3 μm in Ge-doped-silica-core fibers (a) as functions of dose for various dose rates and (b) as functions of time following removal from the source. Symbols and noisy curves are data. Straight lines in (a) are power-law behaviors drawn for comparison purposes. Smooth curves in (b) are theoretical predictions (see text). $T=-55\,^{\circ}\text{C}$ for data at the higher dose rates; $T=-20\,^{\circ}\text{C}$ for the lowest.

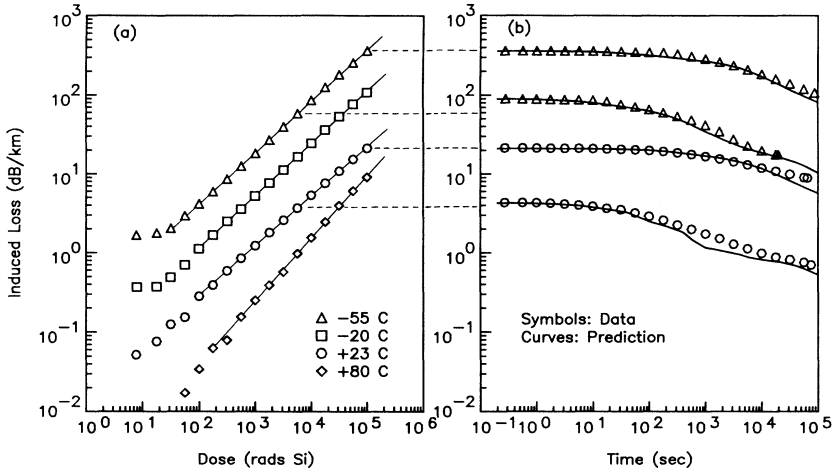

FIG. 3. γ-ray-induced losses at 1.3 μm in Ge-doped-silica-core fibers (a) as functions of dose at various temperatures for a fixed dose rate $\dot{D}=28$ rad/s and (b) as functions of time following removal from the source. Symbols are data. Straight lines in (a) are power-law behaviors (from top to bottom, $f=0.64$, 0.66, 0.63, 0.78) drawn for comparison purposes. Smooth curves in (b) are theoretical predictions (see text). Separate fiber samples were used to obtain decay curves following cumulative doses of 5 and 100 krads.

the correctness of the model, while promising to be of considerable practical value for extrapolating the performances of optical fibers in varied radiation environments from a limited data set.

With the phenomenological model thus established, it is desirable to seek a deeper physical understanding of the set (or continuum) of defect subpopulations characterized by the rate-constant pairs (K_i,R_i). The temperature dependence data of Fig. 3(a) show that the R_i, at least, must be thermally activated. It is our sense that the K_i cannot have a temperature dependence, since the energy spectrum of the inducing γ rays, peaking near 1.5 MeV, must surely dominate. Therefore, to develop Arrhenius plots from the data of Fig. 3(a), we used Eq. (8) to calculate $R_i(T)$ for each of several K_i values defined by the passing parallel lines K_iD through the four experimental data sets. (It would be incorrect to use any group of four temperature points at some fixed dose, since each of these would belong to a different K_i value.) The plots so obtained, corresponding to K_i values of 0.0003, 0.001, 0.005, and 0.02 dB/km/rad, yielded activation energies of 1.14, 1.35, 1.15, and 1.01 eV, respectively. These values are in excellent agreement with the activation energy of 1.17 eV [16] for diffusion of O_2 molecules in silica glass and are much higher than the activation energies of any other known atomic, molecular, or electronic species in silica. Since it is known (1) that GeO_2 is more easily reduced to the monoxide than is SiO_2, (2) that O_2 molecules can be produced radiolytically even in pure a-SiO_2 [17], and (3) that O_2 has a so-called "atmospheric absorption band" at 1.27 μm [18], we regard O_2 molecules as the radiation product most likely responsible for the measured attenuations at 1.3 μm as well as the mobile species determining the recombination kinetics. We speculate that the existence of a range of subpopulations is a manifestation of spatially correlated O_2/oxygen-divacancy pairs in a range of initial separations, with the closest pairs being produced (and recombining) at the greatest rates. We assume without proof that the intermediate-range order of the glass network enters in determining the precise dependence of R_i on K_i, Eq. (7). In this interpretation, there must exist *nearest-neighbor* pairs which would define upper bounds on the distributions of K_i and R_i. This notion is supported by the data of Fig. 2(a), where the dashed straight line—representing an initially observed *linear* response at the highest dose rate—can be interpreted as $K_{\max}\approx 0.07$ dB/km/rad.

We note in passing that other explanations for specific power-law growth behaviors have been posited. For example, it has been pointed out [11] that a $D^{1/2}$ behavior can result from a quasi-mass-action law if a primary defect produced linearly with dose were to reversibly dissociate into two daughter defects which become the measured quantities. However, this special case would require that the decay time of the primary defect (and hence the daughter defects in equilibrium with it) be long with respect to the longest irradiation times over which the power-law behavior can be observed. By contrast, our model predicts—and the present data show—decay times comparable to the irradiation times, t_{irrad}, over the entire range of power-law behavior.

We have supposed that the exponent α in Eq. (1) may be related to the exponent f in Eq. (2). On the basis of our analysis, the relation $\alpha=1-f$ (as opposed to $\alpha=f$) is at least qualitatively correct for postirradiation times $t>t_{\text{irrad}}$ and $1>f>0$. In Fig. 4, we compare data from Fig. 2(b) with no-adjustable-parameter curves (dashed lines) generated from Eq. (1) using this assumption and

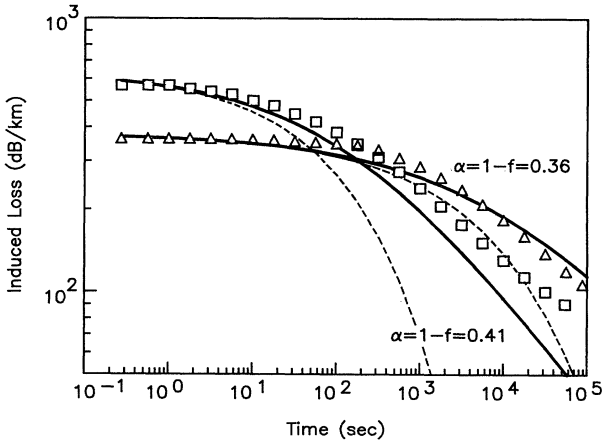

FIG. 4. Data (symbols) from Fig. 2(b) are compared with predictions based on Eq. (1) (dashed curves) and Eq. (10) (bold curves) using $\alpha=1-f$ and $1/\tau=(1-f)/t_{\text{irrad}}$, where f is taken from Fig. 2(a) [19].

taking $1/\tau \equiv R=(1-f)\dot{D}D^{-1}=(1-f)/t_{\text{irrad}}$ as derived from the present theory for $n=1$. It is seen that these Kohlrausch curves deviate significantly from the data at long times. The bold, fully drawn curves in Fig. 4 are analogous no-adjustable-parameter "stretched second-order solutions"

$$q(t)=q_0[1+(t/\tau)^{\alpha}]^{-1}, \tag{10}$$

again assuming $\alpha=1-f$ and taking $1/\tau \equiv q_0 R=(1-f)\dot{D}D^{-1}=(1-f)/t_{\text{irrad}}$ from Eqs. (2), (8), and (9). Although better agreement with the data could be achieved by freely varying all parameters in any one of Eqs. (1), (9), or (10), no added physical intuition would accrue. By contrast, the present parametrization of Eq. (10) is understandable in terms of the above analysis and offers a practical approximation for *predicting* the bimolecular decay kinetics of defect populations exhibiting well-formed [19] power-law growth curves.

[1] R. Kohlrausch, Ann. Phys. (Leipzig) **12**, 393 (1847).

[2] K. L. Ngai, Comments Solid State Phys. **9**, 127 (1979); **9**, 141 (1979).

[3] R. W. Rendell and K. L. Ngai, in *Relaxations in Complex Systems,* edited by K. L. Ngai and G. B. Wright (National Technical Information Service, Springfield, VA, 1984), p. 309.

[4] R. G. Palmer, D. L. Stein, E. Abrahams, and P. W. Anderson, Phys. Rev. Lett. **53**, 958 (1984); **54**, 1965 (1985).

[5] A. I. Gusarov, A. V. Dmitryuk, A. N. Kononov, and V. A. Mashkov, Zh. Eksp. Teor. Fiz. **97**, 525 (1990) [Sov. Phys. JETP **70**, 289 (1990)].

[6] R. L. Pfeffer, J. Appl. Phys. **57**, 5176 (1985).

[7] R. A. B. Devine and J. Arndt, Phys. Rev. B **39**, 5132 (1989).

[8] D. L. Griscom, Nucl. Instrum. Methods Phys. Res., Sect. B **46**, 12 (1990).

[9] E. J. Friebele, C. G. Askins, C. M. Shaw, M. E. Gingerich, C. C. Harrington, D. L. Griscom, T. E. Tsai, U. Paek, and W. H. Schmidt, Appl. Opt. **30**, 1944 (1991).

[10] E. J. Friebele, M. E. Gingerich, and D. L. Griscom, *Optical Materials, Reliability and Testing: Benign and Adverse Environments,* SPIE Proceedings Vol. 1791 (SPIE, Bellingham, WA, 1993), p. 177.

[11] H. Imai *et al.* (to be published).

[12] Spectran SG320R, graded index 100 μm core, 140 μm clad.

[13] Reference [5] treats radiation-induced defects detected by electron spin resonance in bulk $NaPO_3$ and $Ca(PO_3)_2$ glasses and reports dose-dependent recovery rates potentially interpretable by the present theory. Although the authors of Ref. [5] described their growth curves as having an initial "linear dose dependence," the straight-line slopes scaled from the illustrated log-log plots were $f=0.85$ and 0.75 for the respective glasses, i.e., they were power laws.

[14] An explicit case can also be made for the inherently natural presumption of second-order kinetics: Inspection of the model solutions of Fig. 1 reveals that the assumption of $n=1$ implies f to be independent of $\dot{D}$ (and $C \propto \dot{D}$), whereas the experimental data of Fig. 2(a) show more complex behavior, with f decreasing with increasing $\dot{D}$.

[15] The roller-coaster natures of the predicted curves result from the crude approximation of using just three subpopulation components, corresponding to the nominal mean K_i value, K_{mean}, plus the components $3K_{\text{mean}}$ and $(1/3)K_{\text{mean}}$.

[16] F. J. Norton, Nature (London) **191**, 701 (1961).

[17] T. E. Tsai and D. L. Griscom, Phys. Rev. Lett. **67**, 2517 (1991).

[18] B. J. Finlayson-Pitts and J. N. Pitts, Jr., *Atmospheric Chemistry: Fundamentals and Experimental Techniques* (Wiley, New York, 1986), p. 139.

[19] The present analysis correctly predicted the half-life [τ in Eq. (10)] in all cases except for the highest-dose-rate data of Fig. 2. The factor-of-2 discrepancy between the experimental and predicted values of τ evident in Fig. 4 (squares) is tentatively ascribed to the continuous curvature (as opposed to straight-line behavior) manifested in the corresponding log-log growth curve of Fig. 2(a).